



City Research Online

City, University of London Institutional Repository

Citation: Guan, Y., Zhang, T., Dong, X., Sun, T. & Grattan, K. T. V. (2023). Sensor for simultaneous measurement of temperature and humidity based on a chirped fiber Bragg grating partially bonded with thick polyimide film. *IEEE Sensors Journal*, 23(20), pp. 24583-24590. doi: 10.1109/jsen.2023.3312067

This is the accepted version of the paper.

This version of the publication may differ from the final published version.

Permanent repository link: <https://openaccess.city.ac.uk/id/eprint/31387/>

Link to published version: <https://doi.org/10.1109/jsen.2023.3312067>

Copyright: City Research Online aims to make research outputs of City, University of London available to a wider audience. Copyright and Moral Rights remain with the author(s) and/or copyright holders. URLs from City Research Online may be freely distributed and linked to.

Reuse: Copies of full items can be used for personal research or study, educational, or not-for-profit purposes without prior permission or charge. Provided that the authors, title and full bibliographic details are credited, a hyperlink and/or URL is given for the original metadata page and the content is not changed in any way.

City Research Online:

<http://openaccess.city.ac.uk/>

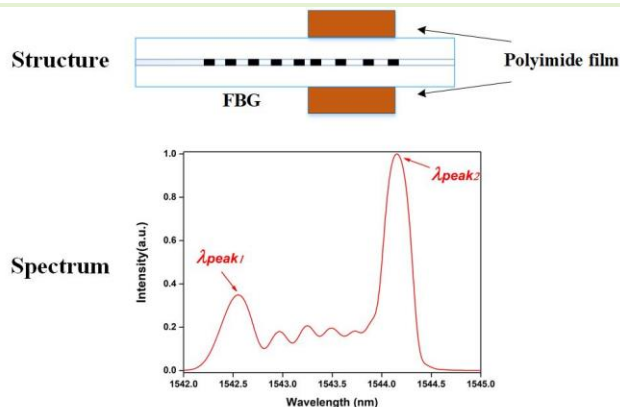
publications@city.ac.uk

Sensor for simultaneous measurement of temperature and humidity based on a chirped fiber Bragg grating partially bonded with thick polyimide film

Yunqing Guan, Ting Zhang, Xiaopeng Dong*, Tong Sun, and Kenneth T. V. Grattan

Abstract—This paper presents a compact fiber-optic sensor based on a fiber Bragg grating (FBG), partially bonded with thick polyimide (PI) films, for the simultaneous measurement of humidity and temperature. Half of the grating was attached to the PI film, while the rest of the grating remained bare. When the sensor was exposed to humidity and temperature changes, a significant non-uniform stress distribution was introduced along the entire grating. The chirp effect occurs, which causes the main peak of the spectrum to split into different peaks. Depending on the wavelength shift of these different peaks, simultaneous measurement of temperature and humidity could be achieved by solving a matrix equation. This is the first time that such a thick PI film-based FBG sensor has been used for humidity and temperature monitoring. The benefit of the approach is that the sub-millimeter thickness of the PI film is *at least one order of magnitude greater* than that of the traditional PI coating used in such sensors. The proposed sensing structure with PI films enhances the sensor response to both humidity and temperature significantly. The humidity and temperature sensitivity are achieved as 13.70 pm/%RH and 19.12 pm/°C, respectively, in the experiment.

Index Terms—dual parameters measurement, polyimide films, chirp effect.



The different peaks present different behaviors to humidity and temperature. Depending on the wavelength shifts of the different peaks, the simultaneous measurement of dual parameters can be achieved through the following matrix.

$$\text{Matrix} \quad \begin{bmatrix} \Delta T \\ \Delta RH \end{bmatrix} = \frac{1}{|k_{T1}k_{RH2} - k_{T2}k_{RH1}|} \begin{bmatrix} k_{RH2} & -k_{RH1} \\ -k_{T2} & k_{T1} \end{bmatrix} \begin{bmatrix} \Delta\lambda_{peak1} \\ \Delta\lambda_{peak2} \end{bmatrix}$$

I. INTRODUCTION

THE simultaneous measurement of temperature and humidity is essential in many of today's applications, such as in agriculture, meteorology, environmental monitoring, and the pharmaceutical industry, for example. Various types of sensors have been developed for this purpose and compared to electrical sensors, optical fiber sensors designed for temperature and humidity sensing are attractive due to the specific advantages they show, such as corrosion resistance especially in high humidity environments, immunity to electromagnetic interference, high sensitivity, and being lightweight in nature [1]-[3]. Now widely used in many optical fiber sensors, the Fiber Bragg Grating (FBG) has the advantages of compact size and ease of multiplexing, techniques which are extensively used in many practical applications of such sensors.

Based on its thermal expansion and the thermo-optic effect, a bare (uncoated) FBG can be used directly to measure

temperature, at the same time being insensitive to humidity. To create such a sensitivity (in order to form the basis of an effective sensor), it is necessary to coat the grating area of the fiber with a moisture-sensitive polymer, such as Polyimide (PI) or polyvinyl alcohol (PVA), to sensitize the fiber to enable it to be used to measure humidity. Thus the shift of the Bragg wavelength which occurs due to the strain applied on the FBG, is, in the case of humidity measurement, induced by the expansion of the polymer coating due to the absorption of moisture [4]-[7]. Nevertheless, most types of moisture-sensitive polymers show a similar type of response in the FBG to that seen from temperature changes. Thus, it is impossible to discriminate between the effects of humidity and temperature by measuring the shift of the Bragg wavelength alone.

To overcome the problem of the cross-sensitivity of the humidity and temperature when an FBG shift is measured, various schemes have been proposed, which can be mainly

This work was supported in part by the National Natural Science Foundation of China under Grant 61775186, in part by the Marine and Fisheries Bureau of Xiamen under Grant 16CZB025SF03.

Xiaopeng Dong, Yunqing Guan and Ting Zhang are with the School of Electronic Science and Engineering, Institute of Lightwave Technology, Xiamen University, Xiamen 361005, China. Xiaopeng Dong is also with Key Laboratory for Optical Communication Device Test of Xiamen.(email:xpd@xmu.edu.cn,yunqingguan_hit@qq.com,[\[150246@stu.xmu.edu.cn\]\(mailto:150246@stu.xmu.edu.cn\)\). Tong Sun is with the School of Mathematics, Computer Science and Engineering, City, University of London, London EC1V 0HB, U.K. \(e-mail: \[t.sun@city.ac.uk\]\(mailto:t.sun@city.ac.uk\)\). Kenneth T. V. Grattan is with the City Graduate School, City, University of London, London EC1V 0HB, U.K., and also with the School of Mathematics, Computer Science and Engineering, City, University of London, London EC1V 0HB, U.K. \(e-mail: \[k.t.v.grattan@city.ac.uk\]\(mailto:k.t.v.grattan@city.ac.uk\)\). Corresponding author: Xiaopeng Dong.](mailto:23120211</p></div><div data-bbox=)

divided into two. The first allows for the use of *two individual sensors* with different humidity and temperature sensitivities [8]-[10], for example, using a bare FBG, in series with an FBG humidity sensor for temperature compensation. However, the accuracy of the measurement made as a result will be significantly affected by the likely non-overlapping locations of the two sensors used, especially in the case of the dramatic changes that are seen in space applications, for example, in temperature and humidity measurement. The second scheme utilizes a sensor using a combination of wavelength and intensity demodulation methods [11]-[13]. While intensity demodulation-based sensors are usually inconvenient to use (in the need for sensor multiplexing) and to consider the disturbance of the light source as well as the environment on the result of the measurement, and thus an additional photodetector may be required to compensate for any optical power fluctuation that occurs in such a scheme.

To solve these problems, a different, and also compact FBG-based sensor, with a partial PI film, is proposed, and which will allow the simultaneous measurement of humidity and temperature, is proposed in this paper. In this design, half of the grating is bonded with the solid PI films, which respond to the changes experienced in humidity and temperature together. The second part of the sensor is the bare grating, which is sensitive *only* to temperature. The thickness of the solid PI film is generally at least an order of magnitude larger than the one of traditional PI coating, which introduces a more obvious non-uniform strain along the entire grating. Consequently, a chirp effect occurs when the proposed sensor was exposed to changes in humidity and temperature in calibration tests. The main peak in the sensor spectrum will split into several new sub-peaks that exhibit different behaviors when exposed to humidity and temperature changes. Thus, to the best knowledge of the authors, this is the first time that the solid *PI films* (as opposed to the more traditional *PI coatings*) were introduced into the fabrication of a combined humidity-temperature sensor, where the enhanced PI thickness is employed to enhance the response, both to humidity and temperature and to allow these to be determined individually.

II. SENSING STRUCTURE AND MEASUREMENT PRINCIPLE

The structure of the sensor designed specifically in this work is shown in Fig. 1(a), and a photograph of the actual sensor is shown in Fig. 1(b). The FBG used in the experiment is made by Anshan Photonics Land Technology Co., Ltd. The grating length of the FBG used in the sensor is 1 cm, with half of the grating bonded with the attached PI film, and the remaining half kept as a bare (uncoated) FBG. The PI film that has been chosen for this work is widely used as a separate film and in photoresists, both being applications exploiting these good, heat-insulating materials, which conveniently are easy to source and inexpensive to purchase. To fabricate the solid PI film, the polyamide acid (PAA) solution is generally selected and uniformly poured onto a continuously running metal belt with a drying chamber. After going through the dry chamber, the dried PAA film is peeled off the metal belt, followed by a series of steps such as drying, quenching, and winding. In Fig. 1(b), the real photo of PI film, whose length, width, and thickness are

5 mm, 5 mm, and 0.1 mm respectively. To avoid the potential for a complex strain transfer process to occur between different materials, a liquid form of PI was used as the adhesive (ensuring that both the film and the adhesive are of the same material and thus show similar responses to temperature and humidity). The FBG used was sandwiched between two pieces of PI film, with adhesive, and then was cured in an oven (at 180 °C for 1 hour) to provide a secure bond between the FBG and the PI material [14].

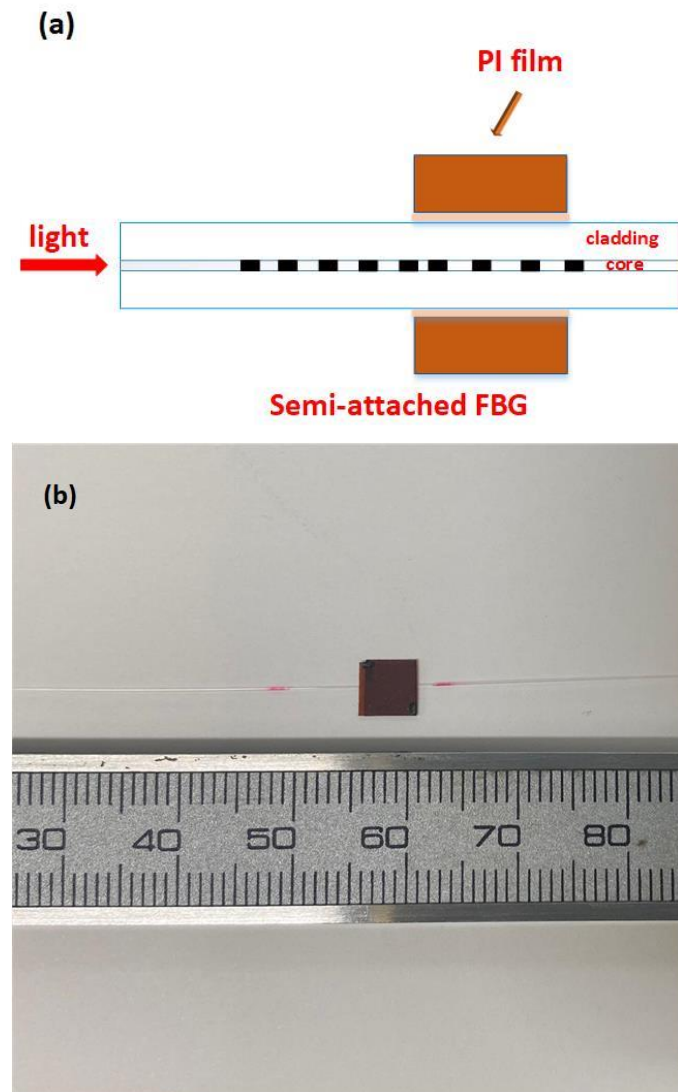


Fig.1. (a) Structure of the sensor. (b) Photograph of the sensor itself.

The optical fiber sensor designed in this way is based on an FBG formed by periodically modulating the refractive index of a fiber core. When broadband light from the source propagates through the grating, the maximum light intensity reflected occurs at the FBG center wavelength λ , which then can be defined as Eq. (1) [15]. The effective refractive index, n_{eff} , and the grating period, Λ , are affected by the measurand, such as strain or temperature, resulting in a wavelength shift from the initial value, λ . When a strain, ϵ , and temperature change, T , occur, the corresponding wavelength shift $\Delta\lambda$ can be expressed as Eq. (2) [14]-[15]. Where p_e is the photoelastic constant of the fiber, α , and ξ are the thermal expansion coefficient and

thermo-optics coefficient of the fiber, respectively, and ΔT is the temperature variation experienced during the experimentation undertaken. In the case of FBG-based humidity sensors designed with PI coated on the area where the gratings were located, the strain induced on the fiber was caused by the swelling of the PI material, arising from exposure to moisture (causing expansion), with further thermal expansion occurring as well. Thus, the total Bragg wavelength shift is given by Eq. (3).

$$\lambda = 2n_{eff}L \quad (1)$$

$$\frac{\Delta\lambda}{\lambda} = (1 - p_e)\varepsilon + [(1 - p_e)\alpha + \xi]\Delta T \quad (2)$$

$$\frac{\Delta\lambda}{\lambda} = (1 - p_e)\varepsilon_{RH} + (1 - p_e)\varepsilon_T + \xi\Delta T \quad (3)$$

The strain, ε_{RH} , caused by the expansion of the PI material due to exposure to moisture can be written as [14],[16]:

$$\varepsilon_{RH} = \left[\frac{A_p E_p}{A_p E_p + A_f E_f} \right] (\beta_{pRH} - \beta_{fRH}) \Delta RH \quad (4)$$

Where A_p and A_f are the cross-sectional areas of the PI coating and fiber itself, while the subscripts p and f represent the references to the PI and the fiber, respectively. Further, E_p and E_f are Young's modulus of the two materials respectively, β_{pRH} and β_{fRH} are the moisture coefficients due to the moisture of the two materials, and ΔRH is the (relative) humidity variation that occurs during the calibration. Since the bare (uncoated) grating does not respond to humidity, β_{fRH} is 0. Similarly, the strain, ε_T , caused by the thermal expansion of the PI material and fiber itself can be expressed as follows [17]-[18]:

$$\varepsilon_T = \left[\frac{A_p E_p}{A_p E_p + A_f E_f} \right] (\alpha_{pT} - \alpha) \Delta T + \alpha \Delta T \quad (5)$$

Where α_{pT} is the thermal expansion coefficient of the PI material. Consequently, when substituting Eq. (4) and Eq. (5) into Eq. (3), this will show that $\Delta\lambda$ will be affected by *both* humidity and temperature changes, and these two parameters cannot be determined by the solution of only one equation (Eq. (3)).

However, if the grating region of the fiber sensor is subjected to a clear non-uniform strain, the original single peak in the FBG spectrum will split into multiple peaks, this being well known as a chirp effect [19]-[20]. If the resultant multiple peaks have *different* responses to humidity and temperature, the resultant parameters ΔRH and ΔT can be determined from the following matrix [21]-[23]:

$$\begin{bmatrix} \Delta T \\ \Delta RH \end{bmatrix} = \frac{1}{|k_{T1}k_{RH2} - k_{T2}k_{RH1}|} \begin{bmatrix} k_{RH2} & -k_{RH1} \\ -k_{T2} & k_{T1} \end{bmatrix} \begin{bmatrix} \Delta\lambda_{peak1} \\ \Delta\lambda_{peak2} \end{bmatrix} \quad (6)$$

Where k_{T1} , k_{RH1} , and k_{T2} , k_{RH2} , are the temperature sensitivity and humidity sensitivity of peak1 and the peak2, respectively, and $\Delta\lambda_{peak1}$ and $\Delta\lambda_{peak2}$ are the wavelength shifts of these two peaks. Looking closely, it is clear from Eq. (4) and Eq. (5) that the magnitude of strain is related (in a positive sense) to the

cross-sectional area of the PI material. The PI film used in the FBG sensor designed in this work has a sub-millimeter thickness, importantly this being at least one order of magnitude *greater* than that of the traditional PI coating used in other humidity sensors (e.g. [14]). As a result, the bare (uncoated) grating part and the other part with the PI film attached respond *differently* to humidity and to temperature changes. The entire grating area was thus subjected to a significant non-uniform strain and, as a result, the FBG spectrum becomes chirped. Depending on the wavelength shift of the different peaks seen and responding to Eq. (6), this allows for the simultaneous measurement of temperature and humidity.

Furthermore, to study the characteristics of the chirped spectrum, a simulation model has been developed by using the software FOGS-BG. In this case, first, the spectrum of a bare FBG (i.e. without a PI film attached) was simulated with the following parameters: the grating length was 1 cm, the grating period was 533.94 nm, and the effective refractive index was 1.446. The normalized spectrum obtained is shown as the black curve on the right-hand side of Fig. 2(d). In this approach, after attaching the PI film to one half of the bare grating, the strain distribution along the entire grating area can be determined, this responding to the relationship seen in Eq. (4). Thus, when the ambient humidity changes, the effect is shown as the red curve in the left-hand side of Fig. 2(b). Consequently, the corresponding normalized spectrum of the chirped FBG can be simulated, and this is shown as the green curve in Fig. 2(e).

By comparing these spectra, the right-hand side peak in the chirped FBG spectrum (termed here Peak 2) remains corresponding to the center wavelength and arises from the bare grating part without the PI film (and thus which is sensitive only to temperature), while the left-hand side peak (termed Peak 1) is seen after the attachment of PI film, (and thus which is sensitive to *both* temperature and humidity). As a result, a simultaneous measurement of humidity *and* temperature can be achieved by measuring the wavelength shifts of Peak 1 and Peak 2, responding to Eq. (6).

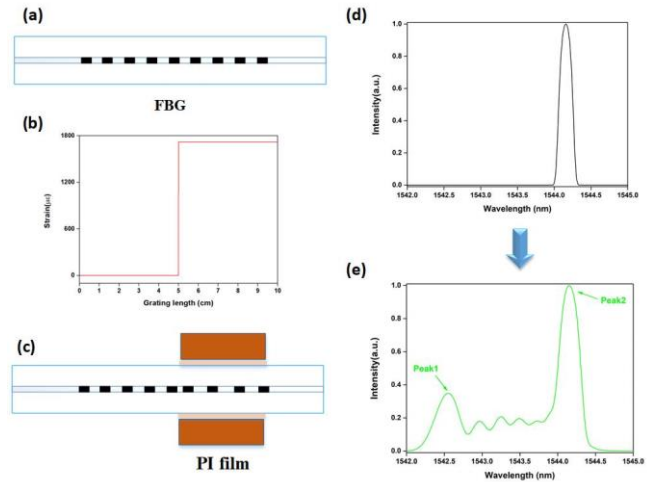


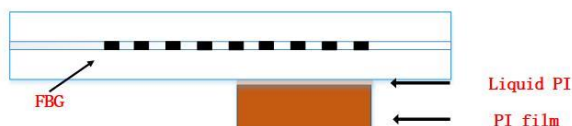
Fig. 2. Comparison of simulated spectra of the bare (uncoated) FBG and the chirped FBG under the non-uniform strain applied. (a) Structure of the bare FBG. (b) Distribution of the strain applied on the FBG. (c) Structure of the sensor. (d) Spectrum of the bare FBG. (e) Spectrum of the chirped FBG.

To fabricate the proposed sensor used in this work, the main steps are listed as follows:

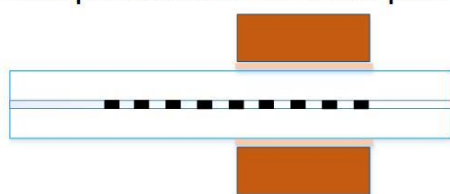
1. Place one piece of PI film on the operation table, then stick it and part of the bare FBG together with the same liquid PI material;
2. Bond another piece of PI film with the first piece, which sandwiches the bare FBG in the middle of the PI films;
3. Put the combination of the FBG and PI films into the oven at 180°C for an hour as the final curing.

For a clearer illustration, the above steps are shown in the following figure.

Step1: Stick part of the FBG on the PI film by liquid PI



Step2: Cover part of the FBG with another piece of PI film



Step3: Curing the FBG and PI films by heat

Fig. 3. The main steps of the fabrication process of the proposed sensor.

III. EXPERIMENTAL RESULTS AND DISCUSSION

Following the fabrication process of the proposed sensor mentioned in section II, the proposed FBG sensor is made. Then, the experimental spectra of the bare FBG and the chirped FBG can be measured, which are shown in Fig.4. The original single peak in the spectrum splits into several sub-peaks, which is consistent with the theoretical analysis. The two peaks in the spectrum can be detected by the peak search algorithm, which finds the relative maximum values in the spectrum.

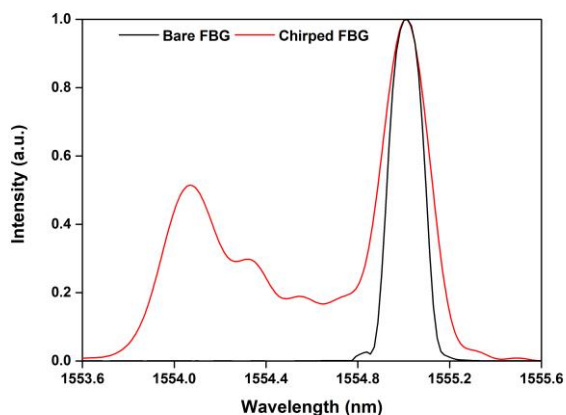


Fig. 4. Comparison of normalized experimental spectra of the bare FBG and the chirped FBG after being bonded with PI films.

To verify the validity of the proposed sensor and to calibrate its performance, an experimental setup was established for the simultaneous measurement of humidity and temperature, as is illustrated in Fig. 5. The light output from a C-band broadband light source is made to propagate to the optical circulator (the insert loss of the circulator is 0.8 dB), which then directed it to

the FBG sensor under test. The response seen in the light reflected from the sensor was monitored using an Optical Spectrum Analyzer (OSA, Yokogawa, AQ6370D). To do so, the sensor was placed in a constant temperature and humidity chamber (Binder, KBF ICH) with a measurement range of 10 %RH to 90 %RH and operating over the temperature range -10 °C to 100 °C.

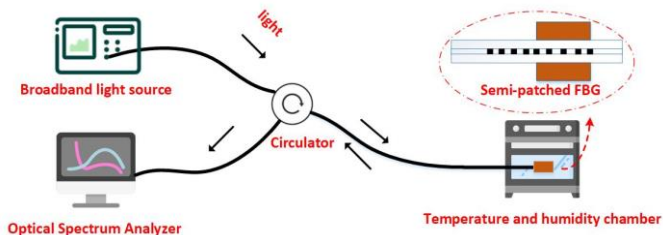


Fig.5. Schematic diagram of the experimental setup for calibration of the sensor for simultaneous measurement of humidity and temperature.

The performance of the sensor to both humidity and temperature changes was evaluated, as discussed below. According to the optimal working range for the temperature and humidity chamber, the humidity measurement range and the temperature measurement range are set as 20 %RH to 60 %RH and 30°C to 70°C, respectively.

A. Humidity Measurement

The sensor was first calibrated to evaluate its performance to changes in humidity, using the setup shown in Fig. 5. To do so, first, the humidity in the chamber was increased from 20 %RH to 60 %RH, this being done at a constant temperature of 30 °C (which is deliberately slightly above the ambient temperature of ~20 °C, to ensure a stable temperature). The results obtained are shown below where Fig. 6(a) depicts the evolution of the normalized spectra from the gratings, with exposure to different humidity values. The data show clearly that Peak1 presents a red shift from 1553.35 nm at 20 %RH to 1553.90 nm at 60 %RH. This leads to a calibration graph, shown in Fig. 6(b), obtained over the same humidity range and showing, from the slope of the graph, a humidity sensitivity of 13.70 pm/%RH. Fig. 6(c) illustrates that the wavelength shift seen for Peak 2 shows a slight fluctuation with humidity change (with a standard deviation in the results of 3.58 pm). It seems likely that this wavelength fluctuation is affected by several factors, such as a lack of uniformity of the PI material and any errors in the fabrication of the sensor which may have occurred. It should be noted that this is very much a laboratory pre-prototype of this design, and further refinement should lead to greater consistency in the production of the sensors using the PI film.

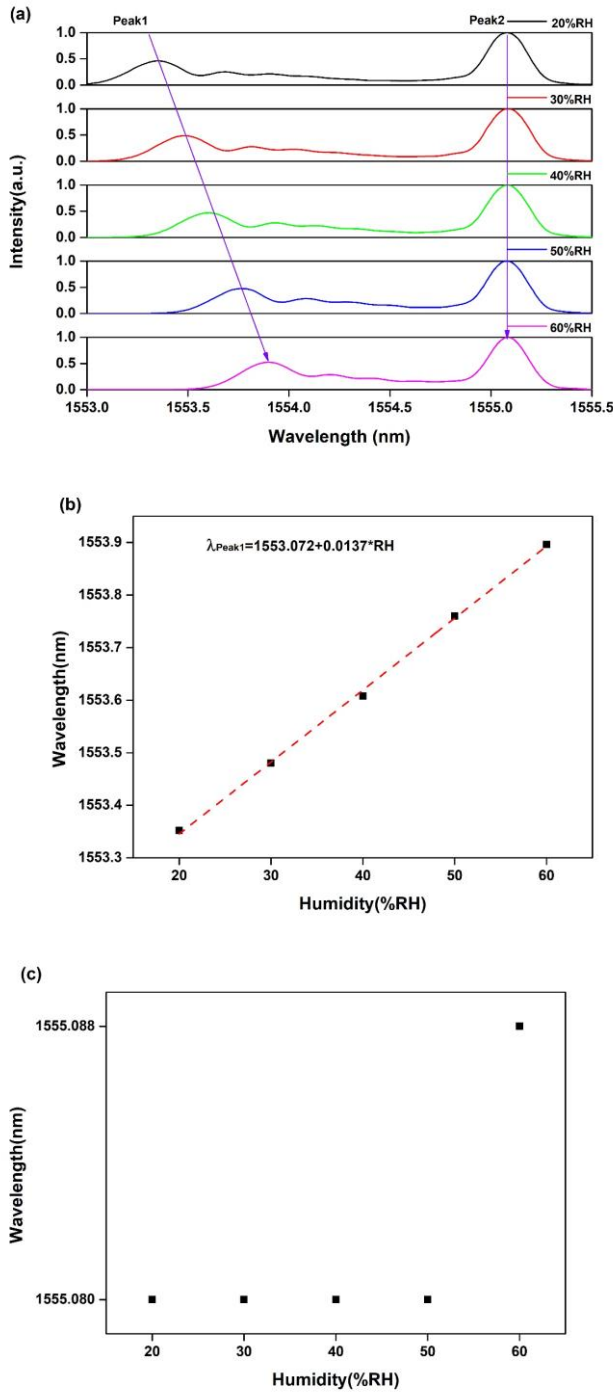


Fig. 6. (a) Experimental spectra obtained when humidity value ranges from 20 %RH to 60 %RH, at a constant temperature of 30 °C. (b) Linear fit of the wavelength shift of Peak 1. (c) Wavelength shift of Peak 2.

B. Temperature Measurement

In the second phase of the experiment, the sensor performance is evaluated at a fixed humidity value in the chamber of 60 %RH, during which the performance of the sensor to changing temperature is evaluated. In the experiment carried out, the temperature increases from 30°C to 70°C, and the normalized spectra obtained are shown in Fig. 7(a). It can be seen from the figure that as the temperature increases, both Peak 1 and Peak 2 exhibit a red shift, with a temperature sensitivity of 19.12 pm/°C and 11.00 pm/°C, respectively. The

calibration graphs based on the above are shown in Fig. 7(b) and Fig. 7(c) for Peak 1 and Peak 2, respectively. The temperature sensitivity of the former is greater than that of the latter because the PI film enhances the response of the FBG, forming the basis of the sensor to temperature change.

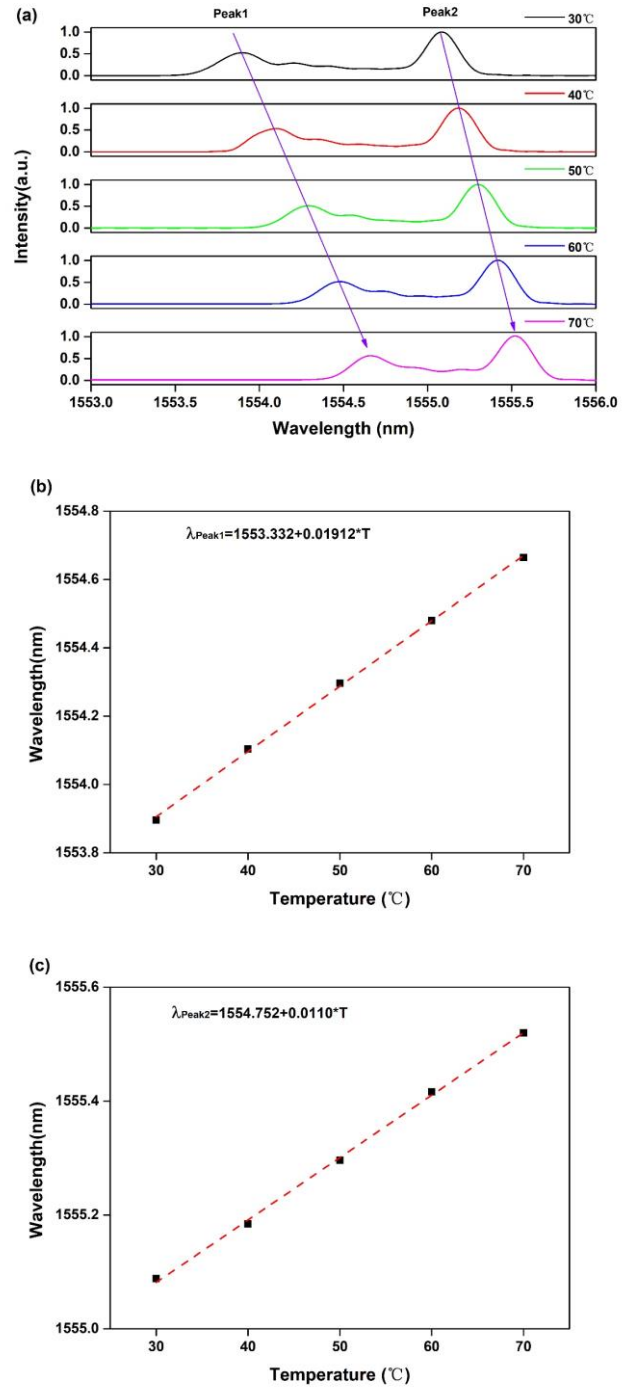


Fig. 7. (a) Experimental spectra obtained when temperature value ranges from 30°C to 70°C, at a constant humidity of 60 %RH. (b) Linear fit of the wavelength shift of Peak 1. (c) Linear fit of the wavelength shift of Peak 2.

Analyzing the above results further, the coefficients in Eq. (6) can be determined to be as follows: $k_{RH1} = 13.70$ pm/%RH; $k_{RH2} = 0$ pm/%RH; $k_{T1} = 19.12$ pm/°C, and $k_{T2} = 11.00$ pm/°C.

Then, the absolute values of the humidity and temperature can be obtained by the following steps:

1. From the experiment result, Peak2 in the spectrum doesn't respond to the humidity variation. Thus, the absolute value of the temperature can be obtained through the wavelength shift of Peak2 and the equation shown in Fig. 7(c).
2. Then, the wavelength shift (represented by ST1) of Peak1 caused by the temperature variation can be calculated, according to the temperature value got in by the former step and the equation shown in Fig. 7(b). The wavelength shift (represented by SH1) of Peak1 caused by the humidity variation can be obtained, according to ST1 and the sum wavelength shift of Peak1. Finally, the humidity value can be calculated according to SH1, and the equation shown in Fig. 6(b).

C. Simultaneous Measurement Of Humidity And Temperature

An important feature of a practical sensor of this type is the simultaneous measurement of humidity and temperature changes that are occurring. To evaluate this, the setup shown in Fig. 5 was used and an experiment was carried out by varying the humidity and temperature conditions. Initially, the temperature of the chamber was set from 30°C to 70°C with an increment of 10°C. Meanwhile, the humidity varied in the range between 30 %RH and 70 %RH. During these experiments, the wavelength shifts of Peak 1 and Peak 2 were monitored. The absolute values of humidity and temperature can be calculated by the method mentioned in the former section, which is represented by the blue dots in Fig. 8. The red lines and green lines indicate the set values of the humidity and temperature chamber. It can be seen that there is a consistent performance, and analysis shows that for *temperature*, the standard deviation is 0.48 °C. By contrast, for *humidity*, a higher standard deviation of 1.48 %RH is seen, reflecting the different sensitivities of the device to these parameters. Above all, the result clearly shows the effectiveness of the sensor described for the simultaneous generation of both humidity and temperature data.

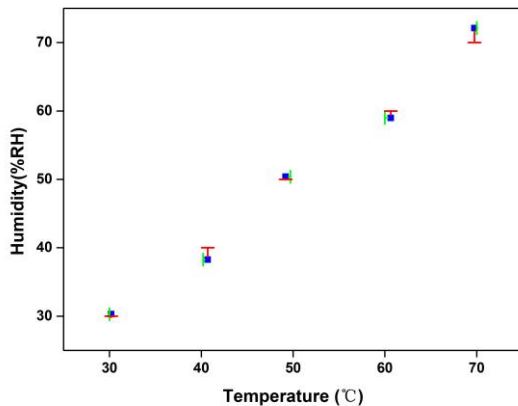


Fig. 8. Sensor response when humidity and temperature change at the same time.

D. The Humidity Response Time

Besides, the humidity response time is also a critical part of the performance of the sensor and it is also investigated. A PI-coated FBG humidity sensor (the thickness of PI is around 40 μm) is fabricated by the traditional coating method (the same

method mentioned in [14]) and is used for comparison. The temperature of the chamber is fixed at 30 °C and the humidity variation is 46 %RH. The wavelength shift of the sensor is measured by a 10 Hz interrogator and the corresponding result is illustrated by the following figure.

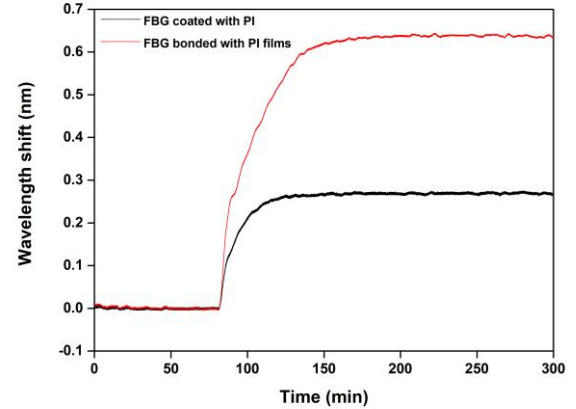


Fig. 9. Comparison of the humidity response time of the proposed sensor and the traditional sensor with PI coating.

From the black line in the figure above, the response time of the traditional PI-coated sensor is approximately 30 minutes, which is similar to the previous result in [14]. In contrast, the proposed sensor, represented by the red line, owns a longer response time, due to the larger thickness of the PI material. Therefore, there is a trade-off between sensitivity and time response when selecting the thickness of the PI film to fabricate the proposed sensor.

E. The Repeatability Of The Sensing Performance

To evaluate the repeatability of the sensing performance of the proposed sensor, we have made another five sensors according to the fabrication process mentioned in Fig. 3. The humidity sensitivity and temperature sensitivity of each sensor are listed in the following table:

TABLE I
THE HUMIDITY SENSITIVITY AND TEMPERATURE SENSITIVITY OF EACH SENSOR.

Sensor id	Humidity sensitivity of Peak1 (pm/%RH)	Temperature sensitivity of Peak1 (pm/°C)	Temperature sensitivity of Peak2 (pm/°C)
1	13.41	18.95	9.28
2	14.71	19.77	12.29
3	15.22	17.97	10.05
4	13.41	19.05	10.70
5	12.73	20.51	10.59

The standard deviations of the humidity sensitivity of Peak1, and temperature sensitivities of Peak1 and Peak2 are 1.03 pm/%RH, 0.95 pm/°C, and 1.11 pm/°C, respectively. The sensitivity difference may lie in the uniformity of the liquid PI material used in the fabrication process of the sensor and the slight temperature difference of different positions in the heating oven. Generally, the repeatability of fabrication and sensing performance of the proposed sensor behaves well, mainly lies in that the PI film, as the main material of the sensor, can already be produced in industrial quantities, while the

traditional PI coating is generally made by the lab's own coating machines.

Furthermore, a comparison of the performance of the proposed sensor, and the ones reported by the existing literature, is shown in the following table.

TABLE II
THE COMPARISON OF DIFFERENT HUMIDITY AND TEMPERATURE OPTICAL FIBER SENSORS.

The structure of the sensor	Humidity sensitivity (pm/%RH)	Temperature sensitivity (pm/°C)	Reference
PI Coated FBG cascaded with a bare FBG	5	11	[24]
The proposed sensing structure	14	19	-
A bare FBG cascaded with Fabry-Perot interferometer	22	10	[9]
Mach-Zehnder interferometer and Fabry-Perot interferometer	-132	370	[8]
Long period gratings array	530	460	[25]

By comparison, the proposed sensor owns much higher humidity sensitivity and temperature sensitivity than that of the FBG-based sensor, thanks to the utilization of solid PI films with larger thicknesses. Although the sensitivities are lower than the ones of the interferometric sensors, the proposed structure is easy to multiplex and owns a much lower manufacturing cost.

IV. CONCLUSION

A novel FBG-based sensor design for the simultaneous measurement of humidity and temperature has been studied theoretically and demonstrated experimentally. In the sensor, the FBG spectrum becomes chirped due to the partial attachment of the PI films used in this design (contrasting with thin PI coatings used in conventional humidity sensors). The separation of the FBG peaks can be calibrated to illustrate the different temperature and humidity behaviors, showing a humidity sensitivity and temperature sensitivity of 13.70 pm/%RH and 19.12 pm/°C. Furthermore, the work suggests that both temperature and humidity sensitivities can be further optimized through the optimization of the thickness of the PI film, an aspect of further work to produce the best sensor based on this design. The major advantage of the design put forward in this work is that the sensor is compact, relatively easy and simpler to fabricate, and potentially low cost. Sensors of this type have great potential for applications, for example in agriculture, metrology, and the biomedical instrumentation industry.

REFERENCES

- [1] C. He, S. Korposh, R. Correia, L. Liu, B. R. Hayes-Gill, and S. P. Morgan, "Optical fibre sensor for simultaneous temperature and relative humidity measurement: Towards absolute humidity evaluation," *Sens. Actuators B Chem.*, vol. 344, Oct. 1, 2021.
- [2] S. Pevec and D. Donlagic, "Miniature all-silica fiber-optic sensor for simultaneous measurement of relative humidity and temperature," *Opt. Lett.*, vol. 40, no. 23, pp. 5646-5649, Dec. 2015.
- [3] Wang, C.L., et al., "Agarose Filled Fabry-Perot Cavity for Temperature Self-Calibration Humidity Sensing," *IEEE Photon. Technol. Lett.*, vol. 28, no. 19, pp. 2027-2030, Oct. 2016.
- [4] X. F. Huang, D. R. Sheng, K. F. Cen, and H. Zhou, "Low-cost relative humidity sensor based on thermoplastic polyimide-coated fiber Bragg grating," *Sens. Actuators B Chem.*, vol. 127, no. 2, pp. 518-524, Nov. 2007.
- [5] D'Amato, R., et al., "Humidity Sensing by Chitosan-Coated Fibre Bragg Gratings (FBG)," *Sensors*, vol. 21, no. 10, May 2021.
- [6] G. Berruti, et al., "Radiation hard humidity sensors for high energy physics applications using polyimide-coated fiber Bragg gratings sensors," *Sens. Actuators B Chem.*, vol. 177, pp. 94-102, Feb. 2013.
- [7] Chai, J., et al., "Optical fiber sensors based on novel polyimide for humidity monitoring of building materials," *Opt. Fiber Technol.*, vol. 41, pp. 40-47, 2018.
- [8] R. J. Tong, Y. Zhao, H. K. Zheng, and F. Xia, "Simultaneous measurement of temperature and relative humidity by compact Mach-Zehnder interferometer and Fabry-Perot interferometer," *Measurement*, vol. 155, Apr. 2020.
- [9] Y. Wang, Q. Huang, W. J. Zhu, and M. H. Yang, "Simultaneous Measurement of Temperature and Relative Humidity Based on FBG and FP Interferometer," *IEEE Photon. Technol. Lett.*, vol. 30, no. 9, pp. 833-836, May 2018.
- [10] S. Q. Zhang, X. Y. Dong, T. Li, C. C. Chan, and P. P. Shum, "Simultaneous measurement of relative humidity and temperature with PCF-MZI cascaded by fiber Bragg grating," *Opt. Commun.*, vol. 303, pp. 42-45, Aug. 2013.
- [11] H. Sun, X. L. Zhang, L. T. Yuan, L. B. Zhou, X. G. Qiao, and M. L. Hu, "An Optical Fiber Fabry-Perot Interferometer Sensor for Simultaneous Measurement of Relative Humidity and Temperature," *IEEE Sens. J.*, vol. 15, no. 5, pp. 2891-2897, May 2015.
- [12] S. N. Wu, G. F. Yan, Z. G. Lian, X. Chen, B. Zhou, and S. L. He, "An open-cavity Fabry-Perot interferometer with PVA coating for simultaneous measurement of relative humidity and temperature," *Sens. Actuators B Chem.*, vol. 225, pp. 50-56, Mar. 2016.
- [13] Qi, Y.F., et al., "Simultaneous measurement of temperature and humidity based on FBG-FP cavity," *Opt. Commun.*, pp. 25-30, Dec. 2019.
- [14] T. L. Yeo, T. Sun, K. T. V. Grattan, D. Parry, R. Lade, and B. D. Powell, "Polymer-coated fiber Bragg grating for relative humidity sensing," *IEEE Sens. J.*, vol. 5, no. 5, pp. 1082-1089, Oct. 2005.
- [15] Hegde, G., et al., "Simultaneous measurement of pressure and temperature in a supersonic ejector using FBG sensors," *Meas. Sci. Technol.*, vol. 33, no. 12, Sep. 2022.
- [16] T. L. Yeo, T. Sun, K. T. V. Grattan, D. Parry, R. Lade, and B. D. Powell, "Characterisation of a polymer-coated fibre Bragg grating sensor for relative humidity sensing," *Sens. Actuators B Chem.*, vol. 110, no. 1, pp. 148-155, Sep. 2005.
- [17] N. A. David, P. M. Wild, and N. Djilali, "Parametric study of a polymer-coated fibre-optic humidity sensor," *Meas. Sci. Technol.*, vol. 23, no. 3, Mar. 2012.
- [18] Alwis, L., T. Sun, and K.T.V. Grattan, "Optical fibre-based sensor technology for humidity and moisture measurement: Review of recent progress," *Measurement*, vol. 46, no. 10, pp. 4052-4074, Dec. 2013.
- [19] S. Kim, S. Kim, J. Kwon, and B. Lee, "Fiber Bragg grating strain sensor demodulator using a chirped fiber grating," *IEEE Photon. Technol. Lett.*, vol. 13, no. 8, pp. 839-841, Aug. 2001.
- [20] O. Frazao, M. Melo, P. V. S. Marques, and J. L. Santos, "Chirped Bragg grating fabricated in fused fibre taper for strain-temperature discrimination," *Meas. Sci. Technol.*, vol. 16, no. 4, pp. 984-988, Apr. 2005.
- [21] C. X. Lu, J. Su, X. P. Dong, T. Sun, and K. T. V. Grattan, "Simultaneous Measurement of Strain and Temperature With a Few-Mode Fiber-Based Sensor," *J. Lightw. Technol.*, vol. 36, no. 13, pp. 2796-2802, Jul. 2018.
- [22] Dey, K., N. Vangety, and S. Roy, "Machine learning approach for simultaneous measurement of strain and temperature using FBG sensor," *Sensor Actuator A Phys.*, vol. 333, Jan. 2022.

- [23] Chaluvadi B., et al., "Recent advancements in fiber Bragg gratings based temperature and strain measurement," *Results Opt.*, vol. 5, Dec. 2021.
- [24] Rente, B., et al., "A Fiber Bragg Grating (FBG)-Based Sensor System for Anaerobic Biodigester Humidity Monitoring," *IEEE Sens. J.*, vol. 21, no. 2, pp. 1540-1547, 2021.
- [25] Hromadka, J., et al., "Simultaneous in situ temperature and relative humidity monitoring in mechanical ventilators using an array of functionalised optical fibre long period grating sensors," *Sens. Actuators B Chem.*, vol. 286, pp. 306-314, May 2019.